NUCLEAR SCIENCE AND TECHNIQUES **26**, 060603 (2015)

Molecular dynamics simulation of displacement cascades in Ni-Mo alloy*

HU Neng-Wen (胡能文),[1,2] QI Mei-Ling (祁美玲),[2] XIAO Shi-Fang (肖时芳),[3]
DENG Hui-Qiu (邓辉球),[3,†] REN Cui-Lan (任翠兰),[4] and HU Wang-Yu (胡望宇)[1,3,‡]

[1]*College of Materials Science and Engineering, Hunan University, Changsha 410082, China*
[2]*Institute of Modern Physics, Chinese Academy of Sciences, Lanzhou 730000, China*
[3]*Department of Applied Physics, School of Physics and Electronics, Hunan University, Changsha 410082, China*
[4]*Shanghai Institute of Applied Physics, Chinese Academy of Sciences, Shanghai 201800, China*
(Received April 22, 2015; accepted in revised form June 9, 2015; published online December 20, 2015)

Molecular dynamics method is used to investigate the displacement cascades in Ni-Mo binary alloy. Effects of the irradiation temperature, energy of the primary knock-on atoms and concentration of solute Mo atoms are taken into consideration on radiation damage to the Ni-Mo alloy. It is found that Mo atoms reduce production of the Frenkel pairs at 100 K, while they enhance defect production at 300 K and 600 K. Size of the largest defect clusters decreases with increasing concentrations of Mo atoms (C_{Mo}) at 100 K, but it increases with C_{Mo} at 300 K and 600 K. Most of the point defects get clustered in cascades leaving only a few vacancies and interstitials isolated.

Keywords: Molecular dynamics method, Displacement cascade, Ni-Mo alloy

DOI: 10.13538/j.1001-8042/nst.26.060603

I. INTRODUCTION

High temperature molten salt reactor (MSR) is one of the most promising and safe type of advanced Generation-IV fission reactors [1, 2]. It is expected to operate with fluoride salt melts as fuels and coolants at high temperatures, which raises several requirements for the structural material candidates, such as high corrosion resistance to fluoride salt melts, good manufacturability, high-temperature strength and sufficient radiation resistance [3]. The use of Hastelloy, especially for Hastelloy N, with Ni and Mo being its predominant compositions, is an important candidate of in-core structural materials in MSR because of their high corrosion resistance to fluoride salt melts, high temperature strength and good manufacturability [4].

Nevertheless, bombardment of energetic particles in materials will induce elastic/inelastic collisions and cause thermodynamics phenomena, such as local heat peak and radiation heat waves in materials [5]. Available experimental results show that ion, electron and neutron can do great damage to the microstructures of Hastelloy to form point defects, dislocation loops, stacking fault tetrahedrons (SFTs), precipitates, which leads to swelling, ductility loss, high-temperature strength degradation, hardening, embrittlement and so on [6–10]. These can severely limit lifetime of MSR. For improving radiation resistance of nickel-based alloy, chemical compositions optimization, which is used currently for commercial alloy, can be an available method [11].

First principle calculation has shown that solute atoms affect cracking properties of Hastelloy N [12], hence the importance of studying the effects of solute atoms on radiation resistance of the alloy. Cascade collisions occur in only a few picoseconds, which is too fast to observe experimentally. Molecular dynamics method has been widely used to study displacement cascade since 1993 [13] when it succeeded in primary damage investigation. It is also widely used to study primary defect behaviors in materials [14–16].

To the authors' knowledge, however, little attentions have been paid on investigation of radiation damage to Ni-Mo alloys [17], especially the displacement cascades in Hastelloy. As the main compositions of Hastelloy N are Ni and Mo atoms [4], we build simple NiMo alloy models in this paper to study effects of irradiation temperature, primary knock-on atom (PKA) energy and contents of solute Mo atoms on the displacement cascades.

II. MODELS AND METHODS

Molecular dynamics method is used to study the displacement cascades in Ni-Mo alloy with modified moldy codes. A set of interatomic potential functions based on the modified analysis embedded atom method (MAEAM) are fitted upon the results of experiments and the first principle calculations. A modified item is added to scale the errors resulting from the spherical approximation of none s-electrons. The total energy of a crystal (E_{tot}) with N atoms can be calculated by

$$E_{\mathrm{tot}} = \sum_i F_i(\rho_i) + \frac{1}{2}\sum_{i,ji\neq j}\phi(r_{i,j}) + \sum_i M_i(P_i), \quad (1)$$

where $\sum_i M_i(P_i)$ is the experiential modification item, $F(\rho)$ is the embedding item, and $\phi(r)$ is the repulsive item. The crossing section describing the interaction between Ni and Mo atoms can be described by

$$\phi_{AB}(r) = \frac{\mu}{2}[\phi_{AA}(C_1 r) + \phi_{BB}(C_2 r)], \quad (2)$$

* Supported by the Strategic Leading Science & Technology Program of the Chinese Academy of Sciences (No. XD02004140), National Natural Science Foundation of China (Nos. 51371080 and 11076012) and Fundamental Research Funds for the Central Universities, Hunan University
† hqdeng@hnu.edu.cn
‡ wyhu@hnu.edu.cn

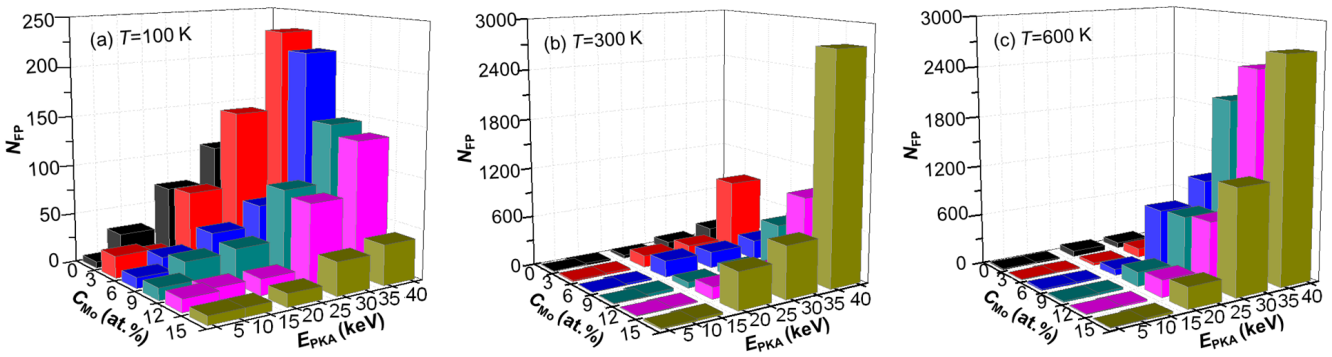

Fig. 1. (Color online) The number of defects generated in displacement cascades caused by PKAs of 5–40 keV in NiMo alloy at (a)100 K, (b)300 K and (c) 600 K.

where μ, C_1 and C_2 are adjustable parameters. The formulae based on MAEAM theory can be found in our previous papers [18]. The information of Ni-Mo binary alloy phase diagram is considered. The formation enthalpies of common stable phases (such as δ-NiMo, D0a and DO22 structural Ni_3Mo and D1a structural Ni_4Mo) are fitted into the crossing interaction potential parameters of Ni and Mo. The Mo solubility in Ni is considered and fitted approximately as 20% at atomic concentration, which agrees well with the phase diagram of Ni-Mo alloy.

Ni-Mo binary alloy models with the solute Mo atoms in concentration ($C_{\rm Mo}$) of 3.0at.%–15at.% are established, where Mo atoms distribute in substitutional sites at random. All alloy models in size of $20a_0 \times 20a_0 \times 20a_0$ are relaxed to equilibrium under the NPT ensemble to obtain the lattice constants at each temperature and concentration of Mo atoms, which last about 250 picoseconds. All displacement cascade simulations are performed in large boxes in size of $60a_0 \times 60a_0 \times 60a_0$ at the temperatures of 100 K, 300 K and 600 K under NVE ensemble, where a_0 is the lattice constant corresponding to the temperature and $C_{\rm Mo}$. The energies of PKAs are 5 keV, 10 keV, 20 keV, 30 keV and 40 keV. In order to avoid tunneling effect, all PKAs are set along the direction of $\langle 135 \rangle$, one of the high index direction. The length of the time step is one femtosecond in general. The total number of time steps for each cascade simulation is 15 000, which lasts about 15 ps. The Wigner-Seitz cell method is adopted to identify defects in each cascade simulations [19]. Another cut-off separation with the length of $1.25a_0$ is used to identify the defect clusters so that two point defects belong to the same defect cluster, if they are within $1.25a_0$ apart. All defects generated in cascade collisions are quenched to 0 K before clustering behavior analysis. Each cascade is run five times for better statistics.

III. RESULTS AND DISCUSSION

The dislocation loops affect the number of defects greatly, so the defects in dislocation loops are excluded in the statistical analysis processes of defect number. The number of defects increases rapidly with the PKA energy, so the PKAs initialized with high kinetic energy cause severe collisions under the NVE ensemble, which may displace a great number of lattice atoms. Therefore more defects will be left in the system after cooling-down of the cascade collisions, though most of the displaced atoms are able to recombine with vacancies.

Figure 1 shows that the number of defects resulting from cascade collisions decreases slightly with increasing atomic concentrations of Mo at 100 K. However, it increases rapidly with $C_{\rm Mo}$ at 300 K and 600 K. Mo atoms seem to play an opposite role in defect generation, They prevent defect generations at low temperatures but enhance them at higher temperatures. This can be understood as synergetic effect of the irradiation temperature and the Mo atom concentration. The randomly distributed solute Mo atoms in Ni-Mo alloy can prevent atoms from both getting displaced and recombining with vacancies in displacement cascade processes. It can be accepted that lattice atoms are harder to get displaced at low temperatures than those at high temperatures because lattice atoms vibrate weaker at low temperature environment than at high temperature. As a consequence, low temperature and high concentration of Mo atoms present an inhibition effect on the defects number. At high temperatures, lattice atoms can be displaced. And once the atoms get displaced, it will be hard for them to get recombined because Mo atoms can prevent displaced atoms from recombining with vacancies, which severely increase the number of defects. In Fig. 1(b), at 300 K, the result at $C_{\rm Mo} = 3.0$at.% and PKA energy $= 40$ keV is abnormal, because of large-sized dislocation loops formed at the stable state, when atoms aggregate and form dislocation loops leaving an amorphous zone in the system. The distribution of cascade defects in NiMo alloy is similar to that in iron and tungsten. Irradiation induced vacancies distribute in the center of cascade region but interstitials migrate to the periphery [20, 21].

Most defects generated in cascade processes distribute in clusters and the number of small cluster increases with PKA energy. Further analysis concerning the distribution of cluster number shows that most of the defect clusters are sized at smaller than 10. And the number of small clusters increases with the PKA energy. Typical results about the cluster num-

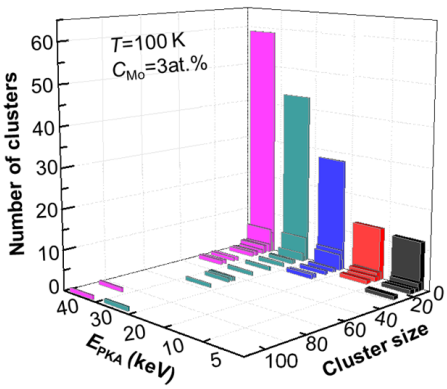

Fig. 2. (Color online) The number of defects cluster as function of the defect cluster size and the PKA energy.

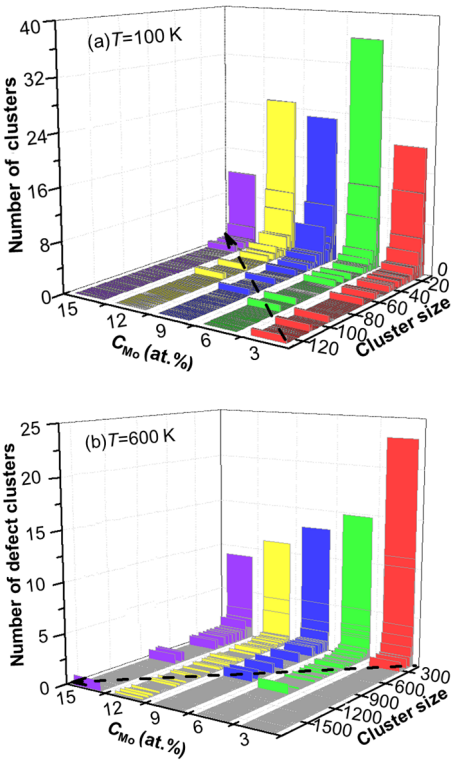

Fig. 3. (Color online) Distribution of defect cluster number as the functions of cluster size and the concentration of solute Mo atoms at 100 K (a) and 600 K(b). The number of defect clusters generated at C_{Mo} =3.0at.% and 100 K includes all clusters formed for each PKA energy.

ber distribution as the functions of PKA energy and cluster size are shown in Fig. 2. The increasing number of small clusters is due to that high energy PKAs may generate high temperature zones, where interstitials and vacancies are easier to migrate and aggregate. The clustering behaviors of cascade defects in Ni-Mo alloy differ from those in Fe-W alloy, where interstitials usually occur in dumbbells, crowdions or sometimes in dislocation loops [22–24]. However, most interstitials cluster into SFTs or interstitial loops and a very little fraction of interstitial atoms keep isolated in Ni-Mo alloy.

The concentration of Mo atoms in Ni-Mo alloy influences the size of the largest cluster, too. As shown in Fig. 3, the number of small clusters decreases slightly with increasing C_{Mo}. The size of the largest clusters in Ni-Mo alloy decreases with increasing atomic concentrations of Mo at 100 K, while it increases sharply with the Mo content at 600 K. This may be due to that the simulation time of cascade process is not long enough for vacancies to migrate to form clusters. Consequently, the formation of small clusters depends on aggregation of interstitial atoms instead of vacancies. Adding more Mo atoms in Ni-Mo alloy reduces the total number of point defects at low temperatures, making interstitials unavailable for cluster-forming, hence the decrease of number of small clusters and size of the largest clusters with increasing C_{Mo}. In high temperature environments, Mo atoms in the systems can increase the number of defects and most of the displaced atoms collapse into dislocation loops. because the time is so limited that they are not able to get recombined. Solute Mo atoms at higher atomic fraction will lead to more interstitials aggregation into loops, which also results in the limited interstitials and decreases the number of small clusters. So, the number of small cluster decreases with increasing C_{Mo}, but the size of the largest clusters increases with C_{Mo}.

IV. CONCLUSION

The effects of solute Mo atoms, irradiation temperature and PKA energy on displacement cascades in Ni-Mo alloy are investigated with the molecular dynamic method. The conclusions can be as follows:

(1) Solute Mo atoms decrease size of the defect clusters. At 100 K, they reduce production of Frenkel pairs; while at 300 K and 600 K they enhance the defect production.

(2) Most point defects get clustered in the cascade processes. Only a few vacancies and interstitials keep isolated. Dislocation loops can form in cascade under high PKA energies and/or high temperatures.

(3) Most vacancies generated in cascade processes stay in the cascade center, which leads to the formation of a poor-atoms zone in cascade region. A small fraction of single point defects and small clusters can form far away from cascade centers.

[1] Mathieu L, Heuer D, Brissot R, *et al*. The thorium molten salt reactor: Moving on from the MSBR. Prog Nucl Energ, 2006, **48**: 664–679. DOI: 10.1016/j.pnucene.2006.07.005

[2] Le Brun C. Molten salts and nuclear energy production. J Nucl Mater, 2007, **360**: 1–5. DOI: 10.1016/j.jnucmat.2006.08.017

[3] Yvon P and Carré F. Structural materials challenges for ad-

vanced reactor systems. J Nucl Mater, 2009, **385**: 217–222. DOI: 10.1016/j.jnucmat.2008.11.026

[4] Bakai A S. Combined effect of molten fluoride salt and irradiation on Ni-based alloys. Mater Issues Gen IV Systems, 2008, 537–557. DOI: 10.1007/978-1-4020-8422-5_27

[5] Ding Y N, Yao Z Y, Miao W Y, *et al*. Experimental observation of radiation heat waves. Nucl Sci Tech, 1997, **8**: 43–45.

[6] Jin S X, Guo L P, Yang Z, *et al*. Microstructural evolution in nickel alloy C-276 after Ar^+ ion irradiation. Nucl Instrum and Meth B, 2011, **269**: 209–215. DOI: 10.1016/j.nimb.2010.12.004

[7] Jin S X, He X F, Li T C, *et al*. Microstructural evolution of P92 ferritic/martensitic steel under Ar^+ ion irradiation at elevated temperature. Mater Charact, 2012, **68**: 63–70. DOI: 10.1016/j.matchar.2012.03.009

[8] Jin S X, Guo L P, Ren Y Y, *et al*. TEM characterization of self-ion irradiation damage in Nickel-base alloy C-276 at elevated temperature. J Mater Sci Technol, 2012, **28**: 1039–1045.DOI: 10.1016/S1005-0302(12)60170-4

[9] Jin S X, Luo F F, Ma S L, *et al*. Evolution of precipitate in nickel-base alloy 718 irradiated with argon ions at elevated temperature. Nucl Instrum Meth B, 2013, **307**: 522–525. DOI: 10.1016/j.nimb.2012.12.105

[10] Wanderka N, Bakai A, Abromeit C, *et al*. Effects of 10 MeV electron irradiation at high temperature of a Ni-Mo-based Hastelloy. Ultramicroscopy, 2007, **107**: 786–790. DOI: 10.1016/j.ultramic.2007.02.029

[11] Rowcliffe A F, Mansur L K, Hoelzer D T, *et al*. Perspectives on radiation effects in nickel-base alloys for applications in advanced reactors. J Nucl Mater, 2009, **392**: 341–352. DOI: 10.1016/j.jnucmat.2009.03.023

[12] Liu W G, Han H, Ren C L, *et al*. The effect of Nb additive on Te-induced stress corrosion cracking in Ni alloy: a first-principles calculation. Nucl Sci Tech, 2014, **25**: 050603. DOI: 10.13538/j.1001-8042/nst.25.050603

[13] Calder A F and Bacon D J. A molecular dynamics study of displacement cascades in α-iron. J Nucl Mater, 1993, **207**: 25–45. DOI: 10.1016/0022-3115(93)90245-T

[14] Chen M and Hou Q. The interaction of defects in titanium: A molecular dynamics study. Nucl Sci Tech, 2010, **21**: 271–274. DOI: 10.13538/j.1001-8042/nst.21.271-274

[15] Caturla M J, Soneda N, Alonso E, *et al*. Comparative study of radiation damage accumulation in Cu and Fe. J Nucl Mater, 2000, **276**: 13–21. DOI: 10.1016/S0022-3115(99)00220-2

[16] Borodin V A and Vladimirov P V. Diffusion coefficients and thermal stability of small helium-vacancy clusters in iron. J Nucl Mater, 2007, **362**: 161–166. DOI: 10.1016/j.jnucmat.2007.01.019

[17] Zhang L and Zhang Z L. Angular distribution of sputtered atoms induced by low-energy heavy ion bombardment. Nucl Sci Tech, 2004, **15**: 340–343.

[18] Wang K, Xiao S F, Deng H Q, *et al*. An atomic study on the shock-induced plasticity and phase transition for iron-based single crystals. INT J Plasticity, 2014, **59**: 180–198. DOI: 10.1016/j.ijplas.2014.03.007

[19] Ashcroft N W and Mermin N D. Solid state physics, In: Saunders, Philadelphia, New Rork (USA): Thomson Learning Inc, 1976, 63–84.

[20] Yang X D, Deng H Q, Hu N W, *et al*. Molecular dynamics simulation of the displacement cascades in tungsten with interstitial helium atoms. Fusion Sci Technol, 2014, **66**: 112–117. DOI: 10.13182/FST13-742

[21] Yang L, Zu X T, Xiao H Y, *et al*. Atomistic simulation of helium-defect interaction in alpha-iron. Appl Phys Lett, 2006, **88**: 091915. DOI: 10.1063/1.2178767

[22] Osetsky Yu N, Bacon D J, Serra A, *et al*. Stability and mobility of defect clusters and dislocation loops in metals. J Nucl Mater, 2000, **276**: 65–77. DOI: 10.1016/S0022-3115(99)00170-1

[23] Wirth B D, Odette G R, Maroudas D, *et al*. Dislocation loop structure, energy and mobility of self-interstitial atom clusters in bcc iron. J Nucl Mater, 2000, **276**: 33–40. DOI: 10.1016/S0022-3115(99)00166-X

[24] Osetsky Yu N, Bacon D J, Gao F, *et al*. Study of loop-loop and loop-edge dislocation interactions in bcc iron. J Nucl Mater, 2000, **283**: 784–788. DOI: 10.1016/S0022-3115(00)00134-3